Geriatrics Gerontology International

DOI: 10.1111/ggi.14940

ORIGINAL ARTICLE

BIOLOGY

Relationship between imaging-derived parameters and circulating microRNAs to study the degree of lung involvement in hospitalized geriatric patients with COVID-19 pneumonia

Sara Cecchini,[1] Mirko Di Rosa,[2] Lorenzo Fantechi,[3] Sara Mecozzi,[1] Giulia Matacchione,[4] Angelica Giuliani,[5] Vladia Monsurrò,[6] Lorenzo Zoppi,[1] Maurizio Cardelli,[7] Roberta Galeazzi,[4] Rina Recchioni,[4] Francesca Marchegiani,[4] Massimo Marra,[8] Jacopo Sabbatinelli,[4,8] Andrea Corsonello,[9] Riccardo Sarzani,[8,10] Antonio Cherubini,[11,8] Anna Rita Bonfigli,[12] Daniela Fornarelli,[3] Enrico Paci,[1] Antonio Domenico Procopio,[4,8] Fabiola Olivieri[4,8] and Giuseppe Bronte[4,8]

[1]Department of Radiology, IRCCS INRCA, Ancona, Italy
[2]Center for Biostatistics and Applied Geriatric Clinical Epidemiology, IRCCS INRCA, Ancona, Italy
[3]Clinical Unit of Nuclear Medicine, IRCCS INRCA, Ancona, Italy
[4]Clinic of Laboratory and Precision Medicine, IRCCS INRCA, Ancona, Italy
[5]Istituti Clinici Scientifici Maugeri IRCCS, Bari, Italy
[6]Department of Medicine, University of Verona, Verona, Italy
[7]Advanced Technology Center for Aging Research, IRCCS INRCA, Ancona, Italy
[8]Department of Clinical and Molecular Sciences (DISCLIMO), Università Politecnica delle Marche, Ancona, Italy
[9]Unit of Geriatric Medicine, IRCCS INRCA, Cosenza, Italy
[10]Internal Medicine and Geriatrics, IRCCS INRCA, Ancona, Italy
[11]Acute Geriatric Unit, Geriatric Emergency Room and Aging Research Centre, IRCCS INRCA, Ancona, Italy
[12]Scientific Direction, IRCCS INRCA, Ancona, Italy

Aim: Chest computed tomography (CT) scan is useful to evaluate the type and extent of lung lesions in coronavirus disease 2019 (COVID-19) pneumonia. This study explored the association between radiological parameters and various circulating serum-derived markers, including microRNAs, in older patients with COVID-19 pneumonia.

Methods: A retrospective analysis was designed to study geriatric patients (≥75 years) with COVID-19 pneumonia, who underwent chest CT scan on admission, and for whom clinical data and serum samples were obtained. To quantify the extent of lung involvement, CT-score, the percentage of healthy lung (HL%), the percentage of ground glass opacity (GGO %), and the percentage of lung consolidation were assessed using computer-aided tools. The association of these parameters with two circulating microRNAs, miR-483-5p and miR-320b, previously identified as biomarkers of mortality risk in COVID-19 geriatric patients, was tested.

Results: A total of 73 patients with COVID-19 pneumonia were evaluable (median age 85 years; interquartile range 82–90 years). Among chest CT-derived parameters, the percentage of lung consolidation (HR 1.08, 95% CI 1.02–1.14), CT-score (HR 1.14, 95% CI 1.03–1.25), and HL% (HR 0.97, 95% CI 0.95–0.99) emerged as significant predictors of mortality, whereas non-significant trends toward increased mortality were observed in patients with higher GGO%. We also found a significant positive association between serum miR-483-5p and GGO% (correlation coefficient 0.28; $P = 0.018$) and a negative association with HL% (correlation coefficient −0.27; $P = 0.023$).

Conclusions: Overall, the extent of lung consolidation can be confirmed as a prognostic parameter of COVID-19 pneumonia in older patients. Among various serum-derived markers, miR-483-5p can help in exploring the degree of lung involvement, due to its association with higher GGO% and lower HL%. **Geriatr Gerontol Int 2024; ••: ••–••.**

Keywords: COVID-19, computed tomography severity score, elderly, microRNA, pneumonia.

Sara Cecchini and Mirko Di Rosa equally contributed to this work.

Correspondence
Angelica Giuliani, PhD, Istituti Clinici Scientifici Maugeri IRCCS, Via Generale Bellomo, 73/75, 70124 Bari, Italy.
Email: angelica.giuliani@staff.univpm.it

Received: 15 March 2024
Revised: 20 June 2024
Accepted: 1 July 2024

Introduction

The coronavirus disease 2019 (COVID-19) pandemic due to severe acute respiratory syndrome coronavirus 2 infection has caused high mortality in populations at risk, such as older adults.[1] The vulnerability of the older population is linked to the physiological effects of aging, which affect the immune function, favoring morbidity and mortality from infectious diseases.[2] Furthermore, frailty is a condition that worsens with age and with COVID-19, mainly in hospitalized older people, who tend to show more evident symptoms of this disease.[3] More advanced ages, chronic heart disease, cerebrovascular disease, and diabetes mellitus are the risk factors for functional decline after 1 year since hospitalization in older patients who developed COVID-19 pneumonia.[4]

Chest computed tomography (CT) plays an important role not only in the diagnosis and management of COVID-19 but it is also indicated in COVID-19-positive patients with associated comorbidities.[5] Chest CT can accurately evaluate the type and extent of lung lesions, through the evaluation of several parameters; that is, ground glass opacities (GGO), consolidations and crazy-paving pattern.[6] Furthermore, during the pandemic, several international studies evaluated the use of the semiquantitative chest CT severity score as a quick and objective tool[7] to quantify the extent of anatomical chest abnormalities, to stratify the patient's risk and to predict the short-term outcome of patients with COVID-19 pneumonia.[8]

Circulating microRNAs (miR) have been proposed as consistent biomarkers for the diagnosis and/or prognosis, as well as for understanding the pathophysiology of a plethora of clinical conditions, including COVID-19.[9,10] Some evidence highlighted the correlation between severe disease and death with impaired pathways related to inflammation, interferon and antiviral responses, organ damage, and cardiovascular failure.[11] MiR deregulation has also been related to COVID-19 severity and mortality.[11,12] The association between miR levels and COVID-19 outcome could provide a novel tool to develop models for the early prediction of different outcomes and severity, thus permitting the development of personalized therapeutic strategies.[11] We recently identified, based on a small RNA sequencing analysis, two new circulating miRs, miR-483-5p and miR-320b, as biomarkers associated with an increased risk of mortality in COVID-19 hospitalized geriatric patients.[13] However, the association between the miR levels and pulmonary conditions in COVID-19 geriatric hospitalized patients was not previously analyzed.

Another promising marker of COVID-19 prognosis is circulating cell-free DNA (cfDNA).[14] Its plasma concentration is generally low in healthy individuals, but its levels increase significantly in several pathological conditions, including tumors and various inflammatory diseases.[15,16]

In COVID-19 patients, plasma cfDNA modulates systemic inflammation, acting as a damage-associated molecular pattern, and its amount correlates with disease progression.[17,18] Recently, we found that cfDNA abundance in the plasma of COVID-19 hospitalized geriatric patients correlates with an important prognostic factor, such as RNAemia, whereas a reduction in another cfDNA-associated parameter, specifically cfDNA integrity, is associated with an increased risk of in-hospital mortality.[19] In the same study, we also found that increased levels of two circulating proteins associated with neutrophil activation (neutrophil elastase, LL-37) and macrophage activation (sCD163) were also associated with increased risk of in-hospital mortality in the same patients.

The aim of the present study was to compare chest CT-derived parameters in COVID-19 pneumonia with a number of circulating innovative biomarkers of immune cell activation/inflammation, including the expression of circulating miRs and cfDNA burden, that we previously identified as mortality risk biomarkers in COVID-19 hospitalized geriatric patients.

Methods

Study design and patient recruitment

The present study is a single-center retrospective analysis carried out on a cohort of patients with COVID-19 pneumonia, who underwent chest CT scan on admission ($n = 197$), and for whom clinical data and serum were obtained ($n = 73$). These patients were recruited in the framework of the Report-Age COVID-19 project, an observational study involving geriatric patients hospitalized for COVID-19 at the Italian National Center on Aging (IRCCS INRCA) between March 2020 and June 2021.

The study was approved by the Ethical Committee of IRCCS INRCA (reference ID: CE-INRCA-20008), and registered under the ClinicalTrials.gov database (reference ID: NCT04348396). The study protocol was carried out according to local and international guidelines and regulations, and the research was conducted in accordance with the Declaration of Helsinki. Among these patients, we selected 73 older adults (age ≥75 years) from the database on the availability of plasma samples and chest CT scan at hospital admission. As baseline clinical characteristics, information on the following comorbidities was collected: distributions of infarction, dementia, chronic kidney disease, hypertension, stroke, chronic obstructive pulmonary disease, atrial fibrillation, cancer, congestive heart failure, diabetes, Charlson Comorbidity Index (classified as a score from 0 to 2) and the median values with interquartile range of oxygen saturation, and days from COVID-19 diagnosis (through a positive reverse transcription polymerase chain reaction assay of a nasopharyngeal swab), contagion (based

on self-reported information) and appearance of symptoms relatable to COVID-19 to admission.

The Clinical Frailty Scale, an ordinal 9-point scale in which the assessor makes decisions about the degree of frailty from clinical data,[20] was used to assess frailty. Patients were scored from 1 "very fit" to 9 "terminally ill," and grouped into three groups based on their frailty scores. Patients who were scored at 1–3 on the Clinical Frailty Scale were defined as not frail (group 1), patients who were scored at 4–6 (group 2) as vulnerable-mildly frail and patients who scored 7–9 (group 3) as severely frail.

Imaging evaluation

All chest CT findings were defined according to the Fleischner Society glossary, and the qualitative evaluation included the presence of the following CT pulmonary abnormalities: GGO, consolidations, crazy-paving pattern, interlobular thickenings, atelectasis, pleural-parenchymal band, bronchiectasis/bronchiolectasis, reticulation, pulmonary nodules and pleural effusion.[21]

To quantify the extent of pulmonary abnormalities, a semi-quantitative visual scoring system (chest CT severity score) was used based on the degree of lung lobe involvement (0: 0%; 1: <5%; 2: 5–25%; 3: 26–49%; 4: 50–75%; 5: >75%; range: 0–5 for each lobe; global score range 0–25).[22] Chest CT severity scores of 0–7, 8–15, and 15–25 were categorized as mild, moderate, and severe involvement, respectively.

Primary image datasets were transferred to the PACS workstation and evaluated using thoracic VCAR software (GE Healthcare, Chicago, IL, USA), a CE-marked medical device originally designed to quantify pulmonary emphysema and recently adapted for quantification of pneumonia lesions in COVID-19.[23] Lung parenchyma was divided by Hounsfield unit intervals in emphysema (−1024/−977), healthy residual lung parenchyma (−976/−703), GGO (−702/−368) and consolidation (−100/5), and the software automatically calculated the healthy lung volume, the GGO, and the consolidation in liters and percentage.

Radiological parameters

Volumetric chest high-resolution CT examinations were acquired in the supine position at full inspiration and without administration of intravenous contrast medium.

Baseline CT scans, carried out at hospital admission, were performed on a 16-slice MDCT scanner (GE BrightSpeed Elite; GE Healthcare). Scanning parameters were 120 kV and 100–200 mA, with a slice thickness of 1.0 mm and a matrix size of 512 × 512 pixels. Images were reconstructed with a sharp reconstruction kernel for parenchyma. The lung window setting was at a window level of −600 Hounsfield units and a window width of 1600 Hounsfield units.

Three- and 6-month follow-up scans were obtained by 16-slice MDCT scanner (Brilliance; Philips, Amsterdam, the Netherlands) with the following parameters: kvp: 140 kvp, mAs: 170, gantry rotation time: 0.5 s and slice thickness: 1 mm. Coronal and sagittal multiplanar reconstructions were also available in all cases.

Blood sample collection

Peripheral venous blood samples were processed within 2 h from collection. Samples for complete blood count were collected in ethylenediaminetetraacetic acid-anticoagulated blood tubes. Specific plasma and serum tubes were centrifuged at 2500 *g* at 4°C for 15 min. Plasma and serum were immediately processed for routine analysis or stored in aliquots of 500 μL at −80°C for subsequent analysis.

Biological parameters

Total white blood cells (WBC), WBC differential, and platelet counts were carried out by standard automated procedures, and the derived indices neutrophil-to-lymphocyte ratio (NLR), derived NLR (calculated as neutrophil count divided by the result of WBC count minus neutrophil count), platelet-to-lymphocyte ratio and lymphocyte-to-monocyte ratio were calculated. Circulating miR levels were analyzed as previously described.[13]

The open-source encyclopedia of RNA interactomes (http://starbase.sysu.edu.cn/index.php) was utilized to locate target genes of miR-483-5p.[24] A stringent threshold of at least three prediction programs was used to filter out target messenger RNAs (mRNAs).

Ingenuity Pathway Analysis (IPA; QIAGEN, Hilden, Germany) was used to explore the experimentally observed high-predicted and moderate-predicted mRNA targets of miR-483-5p (Table S1) through the miR target filter analysis. Targets were predicted using the TargetScan algorithm by searching for the presence of conserved 8mer and 7mer sites that match the seed region of the miR. Experimentally demonstrated miR/mRNA were identified using content from TarBase with miRBase identifiers. Biological functions and diseases were assessed using IPA software.

The plasma levels of neutrophil elastase, the serum levels of CD163 and circulating nucleic acids were measured following the same procedure described in a previous publication.[19]

Statistical analysis

Regarding descriptive statistics, normality in distribution for continuous variables was assessed by the Shapiro–Wilk test; the mean and standard deviation or median and interquartile range were reported on the basis of their distribution. Comparison of variables between groups was carried out by unpaired Student's *t*-test or Mann–Whitney *U*-test, as appropriate. Categorical variables are expressed as absolute number and percentage, and statistical significance was assessed by the χ^2-test. Imaging-derived parameters (i.e. CT Score, percentage of healthy lung [HL%], GGO% and percentage of consolidation) were dichotomized into under the median or above (or equal to) the median of the variable itself. The association of imaging-derived parameters with mortality during hospital stay was explored by Kaplan–Meier curves and assessed by the log-rank test of equality. Hazard ratios (HR) and 95% confidence intervals (95%CI) were estimated by fitting four Cox proportional hazard models and adjusted for age and sex. To verify the possible association among biological and imaging-derived parameters, Spearman's rank correlation coefficients for all pairs of variables with a $P < 0.01$ were calculated, reporting correlation coefficients (rho) and significance levels (*P*). For statistically significant correlations, two-way scatterplots with regression lines were drawn. A two-tailed *P*-value <0.05 was considered significant. Data were analyzed using Stata version 15.1 Statistical Software Package for Windows (StataCorp, College Station, TX, USA).

Results

Association between clinical and blood-based parameters with lung involvement and survival

Overall, 73 patients (median age 85 years, interquartile range 82–90 years, female to male ratio was 1.35) with COVID-19

pneumonia were evaluable with chest CT scan and blood sample withdrawn on admission. Demographic and clinical characteristics of the study population and after stratifying by survival status are reported in Table 1. A total of 30% (22/73) of the enrolled patients died during the in-hospital stay. Patients who died were significantly older and experiences a high rate of stroke events ($P = 0.002$) and chronic obstructive pulmonary disease ($P = 0.002$). The prevalence of diabetes was higher among survived patients (33.3% vs. 4.5%). Total lung volume and the proportion of healthy lung parenchyma (HL) were higher in survivors, whereas the proportion of lung parenchyma showing consolidation was higher in the group of patients who died.

We then explored the association of chest CT-derived parameters with the hematological parameters WBC, neutrophils, lymphocytes, monocytes, platelet, NLR, derived NLR, platelets, lymphocyte-to-monocyte ratio, and the serum biomarkers miR-483-5p, miR-320b, cfDNA, CD163 and elastase (Table 2).

We found a statistically significant association between the radiological parameters HL%, GGO% and LC% and some clinical characteristics, but no blood-based characteristics. For instance, a higher proportion of women were observed among patients with low CT scores. A high CT score was associated with a longer time from contagion and from symptoms to admission. A low HL% was associated with more frequent chronic kidney disease, stroke, and moderate–severe CT severity. A high GGO% and high LC% were both associated with more frequent chronic kidney disease and moderate–severe CT severity. Deceased patients also more frequently showed stroke, chronic obstructive pulmonary disease and shorter time from infection to admission, but less frequently had diabetes. Furthermore, deceased patients presented with higher WBC and lower monocyte counts.

Table 1 Patients' characteristics according to survival status

	Total $n = 76$	Survived $n = 54$	Deceased $n = 22$	*P*-value
Female sex, *n* (%)	44 (57.9%)	31 (57.4%)	13 (59.1%)	0.893
Infarction, *n* (%)	7 (9.2%)	4 (7.4%)	3 (13.6%)	0.394
Dementia, *n* (%)	23 (30.3%)	17 (31.5%)	6 (27.3%)	0.717
CKD, *n* (%)	14 (18.4%)	8 (14.8%)	6 (27.3%)	0.204
Hypertension, *n* (%)	50 (65.8%)	36 (66.7%)	14 (63.6%)	0.801
Stroke, *n* (%)	10 (13.2%)	3 (5.6%)	7 (31.8%)	**0.002**
COPD, *n* (%)	10 (13.2%)	3 (5.6%)	7 (31.8%)	**0.002**
Atrial fibrillation, *n* (%)	20 (26.3%)	13 (24.1%)	7 (31.8%)	0.487
Cancer, *n* (%)	16 (21.1%)	13 (24.1%)	3 (13.6%)	0.311
CHF, *n* (%)	22 (28.9%)	14 (25.9%)	8 (36.4%)	0.363
Diabetes, *n* (%)	19 (25%)	18 (33.3%)	1 (4.5%)	**0.009**
Charlson Comorbidity Index, *n* (%)				0.856
0	38 (50.0%)	26 (48.2%)	12 (54.6%)	
1	24 (31.6%)	18 (33.3%)	6 (27.3%)	
2	14 (18.4%)	10 (18.5%)	4 (18.2%)	
Clinical frailty scale category, *n* (%)				**0.003**
0–3	15 (19.7%)	14 (25.9%)	1 (4.5%)	
4–6	42 (55.3%)	32 (59.3%)	10 (45.5%)	
7–9	19 (25.0%)	8 (14.8%)	11 (50.0%)	
CT severity, *n* (%)				0.167
Mild (<8)	38 (50%)	29 (53.7%)	9 (40.9%)	
Moderate (9–15)	31 (40.8%)	22 (40.7%)	9 (40.9%)	
Severe (>15)	6 (7.9%)	2 (3.7%)	4 (18.2%)	
NA	1 (1.3%)	1 (1.9%)	0 (0%)	
Age, median (IQR)	86 (82–90)	85 (82–90)	90 (87–93)	**0.003**
Saturation, median (IQR)	97 (95–98)	97 (95–98)	97 (95–98)	0.826
Days from COVID-19 diagnosis to admission, median (IQR)	2 (0–3)	2 (0–3)	1 (0–1)	**0.025**
Days from contagion to admission, median (IQR)	10 (8–14)	11 (8–14)	8 (8–17)	0.574
Days from symptoms to admission, median (IQR)	5 (1–8)	5.5 (1–8)	4 (1–8)	0.815
Duration of hospital stay (days), median (IQR)	14 (9–19)	14.5 (12–20)	9 (4–17)	**0.006**
CT total score, median (IQR)	8 (5.5–12)	8 (5–11)	10.5 (6–15)	0.143
HL (l), median (IQR)	1.5 (1.0–2.3)	1.8 (1.1–2.5)	1.1 (0.7–2.0)	**0.046**
GGO (l), median (IQR)	0.9 (0.6–1.2)	0.9 (0.6–1.2)	0.8 (0.5–1.2)	0.388
Consolidation (l), median (IQR)	0.2 (0.1–0.3)	0.2 (0.1–0.3)	0.3 (0.1–0.4)	0.238
Lung volume (l), median (IQR)	2.8 (2.2–3.5)	2.9 (2.4–3.8)	2.5 (1.7–2.9)	**0.018**
HL (%), median (IQR)	59.9 (38.5–72.8)	61.0 (42.8–72.8)	45.0 (35.8–70.5)	0.254
GGO (%), median (IQR)	32.5 (21.1–46.4)	30.7 (22.7–45.3)	38.5 (19.6–48.7)	0.590
Consolidation (%), median (IQR)	7.5 (4.2–13.6)	6.7 (3.5–11.7)	10.0 (4.9–16.8)	**0.050**

Data are median (interquartile range) or number (%). *P*-values for Mann–Whitney *U*-test (continuous variables) or χ^2-test (categorical variables). CHF, congestive heart failure; CKD, chronic kidney disease; COPD, chronic obstructive pulmonary disease; CT, computed tomography; GGO, ground glass opacity; HL, healthy lung; IQR, interquartile range; NA, not available. *P*-values <0.05 are in bold.

Table 2 Patients' characteristics according to computed tomography score, healthy lung, ground glass opacity and lung consolidation

	Total	CT score			HL			GGO			LC		
		Low	High	*P*	Low HL	High HL	*P*	Low	High	*P*	Low	High	*P*
Clinical characteristics	$n = 73$	$n = 37$	$n = 36$		$n = 37$	$n = 36$		$n = 37$	$n = 36$		$n = 37$	$n = 36$	
Female sex, *n* (%)	42 (57.5%)	26 (70.3%)	16 (44.4%)	**0.026**	22 (59.5%)	20 (55.6%)	0.736	22 (59.5%)	20 (55.6%)	0.736	23 (62.2%)	19 (52.8%)	0.417
Infarction, *n* (%)	7 (9.6%)	4 (10.8%)	3 (8.3%)	0.716	2 (5.4%)	5 (13.9%)	0.218	5 (13.5%)	2 (5.6%)	0.248	5 (13.5%)	2 (5.6%)	0.248
Dementia, *n* (%)	22 (30.1%)	14 (37.8%)	8 (22.2%)	0.146	14 (37.8%)	8 (22.2%)	0.146	9 (24.3%)	13 (36.1%)	0.273	12 (32.4%)	10 (27.8%)	0.665
CKD, *n* (%)	13 (17.8%)	5 (13.5%)	8 (22.2%)	0.331	10 (27.0%)	3 (8.3%)	**0.037**	3 (8.1%)	10 (27.8%)	**0.028**	3 (8.1%)	10 (27.8%)	**0.028**
Hypertension, *n* (%)	48 (65.8%)	22 (59.5%)	26 (72.2%)	0.251	25 (67.6%)	23 (63.9%)	0.741	23 (62.2%)	25 (69.4%)	0.512	22 (59.5%)	26 (72.2%)	0.251
Stroke, *n* (%)	9 (12.3%)	4 (10.8%)	5 (13.9%)	0.689	8 (21.6%)	1 (2.8%)	**0.014**	2 (5.4%)	7 (19.4%)	0.068	2 (5.4%)	7 (19.4%)	0.068
COPD, *n* (%)	10 (13.7%)	6 (16.2%)	4 (11.1%)	0.526	5 (13.5%)	5 (13.9%)	0.963	5 (13.5%)	5 (13.9%)	0.963	4 (10.8%)	6 (16.7%)	0.467
Atrial fibrillation, *n* (%)	19 (26%)	10 (27%)	9 (25%)	0.844	9 (24.3%)	10 (27.8%)	0.737	10 (27%)	9 (25%)	0.844	7 (18.9%)	12 (33.3%)	0.161
Cancer, *n* (%)	15 (20.5%)	8 (21.6%)	7 (19.4%)	0.818	7 (18.9%)	8 (22.2%)	0.727	9 (24.3%)	6 (16.7%)	0.418	9 (24.3%)	6 (16.7%)	0.418
CHF, *n* (%)	22 (30.1%)	12 (32.4%)	10 (27.8%)	0.665	14 (37.8%)	8 (22.2%)	0.146	9 (24.3%)	13 (36.1%)	0.273	11 (29.7%)	11 (30.6%)	0.939
Diabetes, *n* (%)	18 (24.7%)	8 (21.6%)	10 (27.8%)	0.542	10 (27%)	8 (22.2%)	0.643	9 (24.3%)	9 (25%)	0.947	7 (18.9%)	11 (30.6%)	0.249
Charlson Comorbidity Index, *n* (%)				0.175			0.169			0.834			0.425
0	38 (52.1%)	18 (48.6%)	20 (55.6%)		18 (48.6%)	20 (55.6%)		19 (51.4%)	19 (52.8%)		19 (51.4%)	19 (52.8%)	
1	23 (31.5%)	10 (27%)	13 (36.1%)		15 (40.5%)	8 (22.2%)		11 (29.7%)	12 (33.3%)		10 (27%)	13 (36.1%)	
2	12 (16.4%)	9 (24.3%)	3 (8.3%)		4 (10.8%)	8 (22.2%)		7 (18.9%)	5 (13.9%)		8 (21.6%)	4 (11.1%)	
CT severity, *n* (%)							**0.042**			**0.024**			**0.002**
Mild (<8)					13 (35.1%)	23 (63.9%)		24 (64.9%)	12 (33.3%)		26 (70.3%)	10 (27.8%)	
Moderate (9–15)					20 (54.1%)	11 (30.6%)		11 (29.7%)	20 (55.6%)		9 (24.3%)	22 (61.1%)	
Severe (>15)					4 (10.8%)	1 (2.8%)		1 (2.7%)	4 (11.1%)		1 (2.7%)	4 (11.1%)	
NA					0 (0.0%)	1 (2.8%)		1 (2.7%)	0 (0%)		1 (2.7%)	0 (0%)	
Age (years), median (IQR)	85 (82–90)	87 (83–91)	85 (82–89)	0.211	85 (83–90)	86 (81.5–91.5)	0.795	87 (82–91)	85 (82.5–89)	0.539	85 (82–91)	85 (82.5–90)	0.951
Saturation, median (IQR)	97 (95–98)	97 (95–98)	96 (95–98)	0.303	96 (95–98)	97 (95–98)	0.370	97 (95–98)	96 (95–97.5)	0.327	97 (96–98)	96 (95–97)	0.054
Days from COVID-19 diagnosis to Admission, median (IQR)	1.5 (0–3)	2 (0.5–3)	1 (0–3)	0.504	2 (0–4)	1 (0–3)	0.292	1 (0–3)	2 (0–4)	0.233	2 (0–3)	1 (0–3)	0.991
Days from contagion to admission, median (IQR)	10 (8–14)	9 (8–11.5)	12 (9–17)	**0.010**	10.5 (8–14.5)	10 (8–13)	0.615	10 (8–13)	11 (8–16)	0.512	10 (8–12.5)	11 (8–16.5)	0.296
Days from symptoms to admission, median (IQR)	5 (1–8)	2 (0.5–5.5)	7 (3–9)	**0.007**	5 (1–8)	4.5 (1–7)	0.752	4 (1–7)	5 (1–9)	0.711	4 (1–7)	5 (1–9)	0.217
Blood-derived characteristics													
WBC, median (IQR)	8.395 (5.53–11.785)	8.26 (5.97–10.73)	9.57 (4.86–12.6)	0.703	7.45 (4.86–10.73)	9.26 (6.32–14.18)	0.175	8.975 (6.155–12.2)	7.67 (4.995–11.18)	0.446	8.23 (4.87–12.2)	8.565 (5.975–11.18)	0.936
Neutrophils ($\times 10^3/\mu L$), median (IQR)	44 (19.945–61)	46 (27.1–67.7)	41.9 (17.84–59.5)	0.405	45.6 (27.1–61.8)	43.5 (18.39–60.2)	0.572	48.3 (20.925–63)	41 (18.82–60.65)	0.745	41.75 (18.135–58.5)	53.3 (19.945–63.8)	0.472
Lymphocytes ($\times 10^3/\mu L$), median (IQR)	1.225 (0.82–1.75)	1.53 (0.97–1.76)	0.98 (0.77–1.51)	0.093	1.13 (0.81–1.85)	1.42 (0.83–1.65)	0.883	1.325 (0.81–1.65)	1.125 (0.825–1.875)	0.722	1.225 (0.82–1.75)	1.18 (0.81–1.71)	0.806
Monocytes ($\times 10^3/mm^3$), median (IQR)	0.52 (0.38–0.65)	0.59 (0.42–0.72)	0.44 (0.35–0.64)	0.096	0.53 (0.38–0.66)	0.49 (0.38–0.65)	0.623	0.495 (0.385–0.645)	0.56 (0.375–0.69)	0.527	0.495 (0.4–0.645)	0.56 (0.365–0.655)	0.815

(*Continues*)

Table 2 Continued

	Total	CT score			HL			GGO			LC		
		Low	High	*P*	Low HL	High HL	*P*	Low	High	*P*	Low	High	*P*
Clinical characteristics	$n = 73$	$n = 37$	$n = 36$		$n = 37$	$n = 36$		$n = 37$	$n = 36$		$n = 37$	$n = 36$	
PLT, median (IQR)	234 (178.5–296.5)	254 (177–301)	231 (180–294)	0.510	233 (182–288)	254 (177–301)	0.663	246.5 (178.5–300.5)	232 (173.5–288.5)	0.465	255.5 (181–301.5)	230 (171.5–288.5)	0.248
NLR, median (IQR)	32.97 (17.45–50.09)	34.33 (16.32–54.29)	31.43 (23.11–44.02)	0.917	34.33 (23.11–51.67)	31.60 (17.24–43.96)	0.619	33.01 (17.45–49.50)	32.88 (18.41–50.09)	0.796	28.69 (16.81–55.79)	36.35 (24.62–46.26)	0.535
dNLR, median (IQR)	−1.15 (−1.20 to −1.09)	−1.15 (−1.20 to −1.09)	−1.17 (−1.22 to −1.06)	0.653	−1.16 (−1.21 to −1.09)	−1.15 (−1.20 to −1.06)	0.602	−1.15 (−1.19 to −1.07)	−1.16 (−1.21 to −1.09)	0.432	−1.15 (−1.20 to −1.07)	−1.15 (−1.21 to −1.09)	0.830
PLR, median (IQR)	190.98 (128.26–289.99)	160.69 (127.43–275.86)	227.56 (141.21–382.28)	0.276	194.31 (134.15–284.82)	187.65 (127.43–328.76)	0.966	190.98 (130.13–283.48)	179.15 (115.59–335.89)	0.883	188.37 (128.26–335.81)	191.18 (125.47–274.14)	0.717
LMR, median (IQR)	2.34 (1.64–3.44)	2.41 (1.64–3.42)	2.20 (1.75–3.44)	0.936	2.12 (1.64–3.25)	2.41 (1.64–3.57)	0.544	2.36 (1.68–3.44)	2.24 (1.52–3.45)	0.777	2.49 (1.62–3.61)	2.10 (1.69–3.12)	0.341
miR-483-5p, median (IQR)	0.08 (0.02–0.22)	0.06 (0.02–0.26)	0.09 (0.02–0.21)	0.589	0.11 (0.04–0.22)	0.04 (0.01–0.21)	0.087	0.05 (0.01–0.09)	0.12 (0.04–0.24)	0.059	0.06 (0.01–0.34)	0.09 (0.03–0.17)	0.795
miR-320b, median (IQR)	0.17 (0.09–0.31)	0.14 (0.08–0.31)	0.18 (0.10–0.28)	0.766	0.18 (0.09–0.24)	0.16 (0.08–0.39)	0.559	0.14 (0.08–0.39)	0.18 (0.10–0.25)	0.930	0.13 (0.08–0.39)	0.18 (0.10–0.25)	0.934
cfDNA (100–300 bp) [pg/μL], median (IQR)	143 (78.2–263)	126 (59.1–260)	178 (82.2–277)	0.431	172 (82.2–282)	126 (52.2–230)	0.164	121.5 (55.65–200.5)	189 (82.2–287)	0.058	131.5 (55.65–225)	175 (80.4–277)	0.269
CD163 (ng/mL), median (IQR)	634 (452–814)	683 (509–821)	606 (351–782)	0.097	626 (457–764)	658.5 (416–840)	0.569	631 (386.5–830.5)	634 (457–787)	0.890	703.5 (475.5–844.5)	616 (452–730)	0.125
Elastase (ng/mL), median (IQR)	115.5 (69.5–188.5)	114.2 (53–188.5)	116.1 (76.35–183.6)	0.627	137.7 (76.7–192.2)	108.35 (42.7–157.85)	0.216	112.7 (43.7–170.7)	129.7 (75.85–192.85)	0.305	112.7 (52.5–170.7)	119.1 (75.85–192.85)	0.497

Data are median (interquartile range) or number (%). *P*-values for Mann–Whitney *U*-test (continuous variables) or χ^2-test (categorical variables).

cfDNA, cell-free DNA; CHF, congestive heart failure; CKD, chronic kidney disease; COPD, chronic obstructive pulmonary disease; COVID-19, coronavirus disease 2019; CT, computed tomography; dNLR, derived indices neutrophil-to-lymphocyte ratio; GGO, ground glass opacity; HL, healthy lung; IQR, interquartile range; LC, lung consolidation; LMR, lymphocyte-to-monocyte ratio; miR, microRNA; NA, not available; PLR, platelet-to-lymphocyte ratio; WBC, white blood cells. *P*-values <0.05 are in bold.

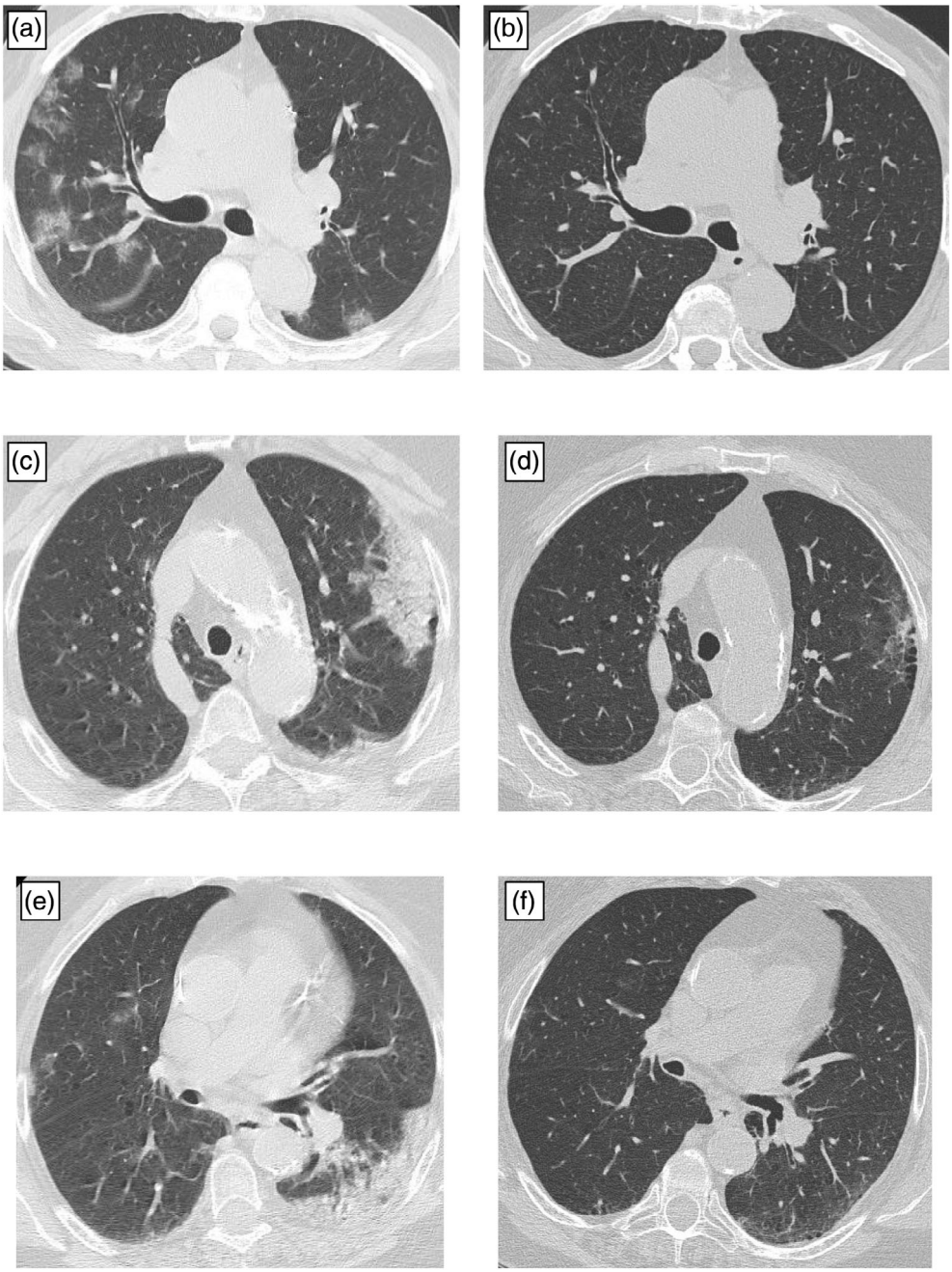

Figure 1 (a, b) Axial thin-section unenhanced chest computed tomography (CT) images in an 81-year-old man who presented with fever, cough and dyspnea. (a) Baseline scan shows multiple bilateral confluent ground glass opacity (GGOs), more numerous on the right lung, with a peripheral distribution; (b) 6-month follow-up scan shows complete resolution of GGOs without fibrosis-like changes. (c–f) Axial thin-section unenhanced chest CT images in a 82-year-old woman who presented with dyspnea. (c, e) Baseline scans show GGOs with superimposed interstitial septa thickening (crazy paving) in the left lower lobe and subpleural consolidative pulmonary opacities in the left upper; (d, f) 6-month follow-up scans show decreased GGOs, interstitial septa thickening and fibrosis-like changes characterized by subpleural parenchymal bands, interstitial septa thickening and honeycombing, and with distortion of lung architecture and thickening of the adjacent pleura.

Figure 1 shows baseline and 6-month CT scans of two older patients who experienced COVID-19 pneumonia.

Prognostic role of radiological parameters

The effect on overall survival of each radiological parameter was tested both as dichotomous and continuous variables. The log-rank test was used to explore the differences in survival time between the patients with high versus low CT score, HL%, GGO % and LC%. Kaplan–Meier curves represented these findings in Fig. 2.

These analyses show a trend toward a better prognosis with low CT score, low GGO%, low LC% and high HL%, even though statistical significance was not reached ($P > 0.05$) in all the four radiological parameters. However, a Cox proportional hazards regression carried out considering these parameters as continuous variables, and adjusting for age and sex showed that LC% (HR 1.10, 95% CI 1.04–1.16) and CT score (HR 1.14, 95% CI 1.03–1.25) were significantly associated with in-hospital mortality. Furthermore, a higher HL% was associated with a decreased risk of mortality (HR 0.97, 95% CI 0.95–0.99). No significant associations were observed for GGO% (HR 1.02, 95% CI 0.99–1.06).

Correlation between radiological parameters and miRs

We also studied the correlation between the four radiological parameters and two biological parameters, miR-483-5p and cfDNA, which achieved $P < 0.1$ in the univariate analysis. These

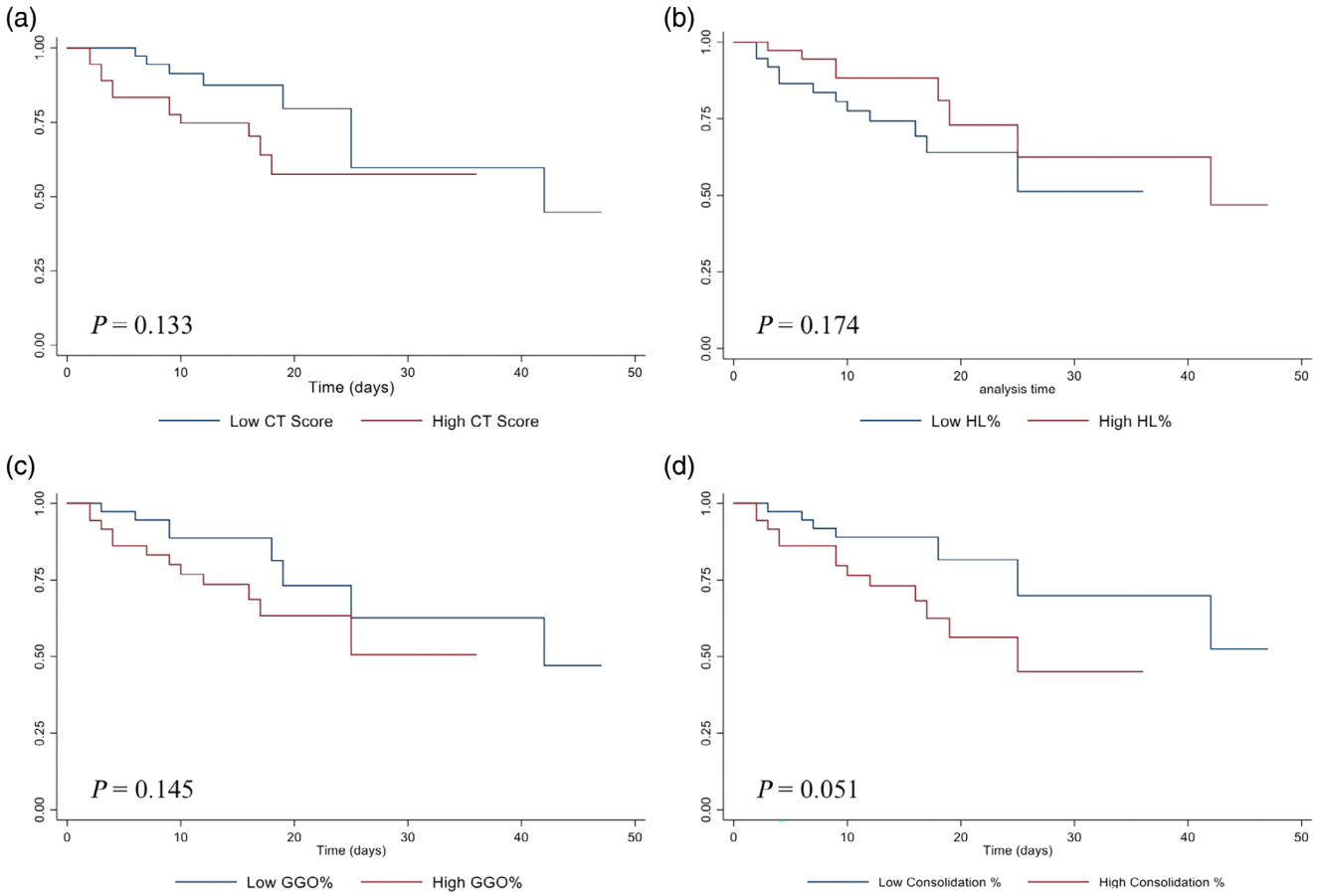

Figure 2 Kaplan–Meier curves of survival time differences between the patients with (a) high versus low computed tomography (CT) score, (b) percentage of healthy lung (HL%), (c) percentage of ground glass opacity (GGO%) and (d) percentage of lung consolidation.

two biological parameters have a higher likelihood of being associated with the risk of COVID-19 in-hospital mortality.[13,19] We verified whether the circulating levels of these two biomarkers are also associated with lung involvement. We found that the levels of miR-483-5p increase with higher GGO% (correlation coefficient 0.28; $P = 0.018$), and decrease with higher HL% (correlation coefficient −0.27; $P = 0.023$; Fig. 3). No correlations were observed between cfDNA and all the radiological parameters (Table S2).

The association of miR-483-5p with the IPA database "diseases and disorders" showed a significant enrichment of biological processes related to lung disease (Fig. 4). All the mRNA targets of miR-483-5p, experimentally observed and highly or moderately predicted, identified by IPA software, are listed in Table S1.

Discussion

In the present cohort study of 73 patients affected with COVID-19 and subjected to chest CT, we investigated the associations between imaging-derived parameters and circulating biomarkers; that is, miRs and cfDNA, previously associated with mortality.

Our results support the prognostic value of CT score and pulmonary involvement, as previously described by other authors,[7,8,25,26] with a significant association between higher LC% and CT score, and lower HL% with increased risk of death.

Similarly, in the present study, the LC% emerged as a feature frequently observed in cases with a worse prognosis, and confirmed its significant negative prognostic role associated with death. Overall, our results are in agreement with previous reports of increased mortality in patients presenting with a reduction of healthy lung parenchyma, as measured using computer-aided tools.[25–27]

In contrast, among the various circulating biomarkers of immune cell activation, including cfDNA and CD163, that we previously analyzed as biomarkers of mortality risk in COVID-19 patients,[19] only miR-483-5p was associated with higher GGO% and lower HL%. However, no correlation was found with LC%.

Recent findings support the involvement of miR-483-5p in infectious diseases. It was found that high levels of miR-483-5p showed >90% sensitivity and specificity in discriminating between adult COVID-19 patients and healthy individuals.[12] In addition, miR-483-5p has been found to be upregulated in pediatric pneumonia, severe pneumonia, and pulmonary TB patients compared with healthy individuals.[28,29] Here and in our previous work,[13] we extended the association between miR-483-5p and COVID-19 clinical and radiological characteristics to older individuals.

In the IPA knowledge database, the diseases and functions predicted to be affected by miR-483-5p in the lung confirm its involvement with lung fibrosis. The present results suggest that miR-483-5p could be implicated in COVID-19 infection by participating in the activation of immunity and the fibrotic process.

It is reasonable to assume that early and intense activation of immunity might find its morphological correlation with GGO%

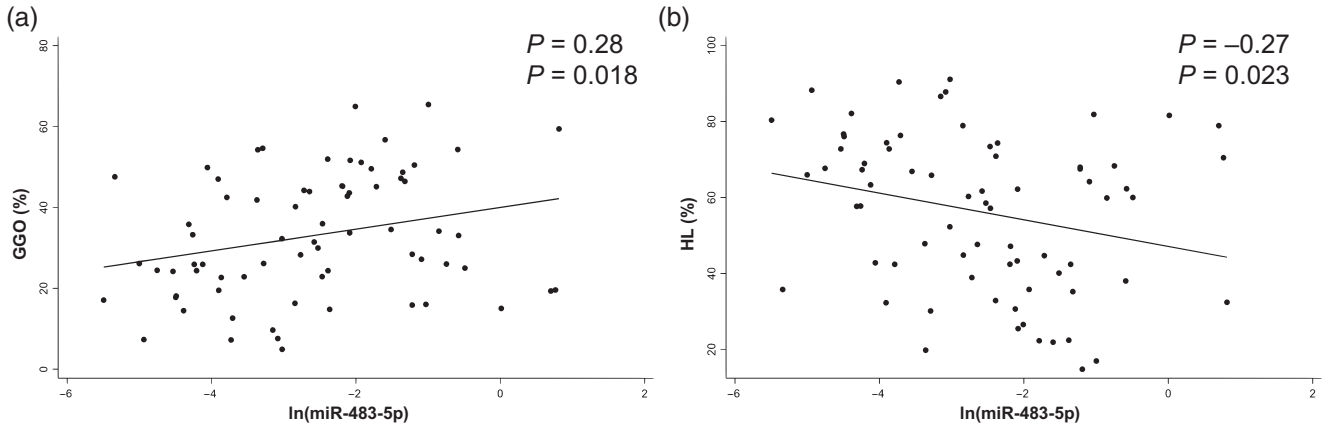

Figure 3 Scatter plots with regression lines of the correlations between microRNA (miR)-483-5p with (a) percentage of ground glass opacity (GGO) and (b) percentage of healthy lung (HL). Spearman's rho coefficients and *P*-values are shown.

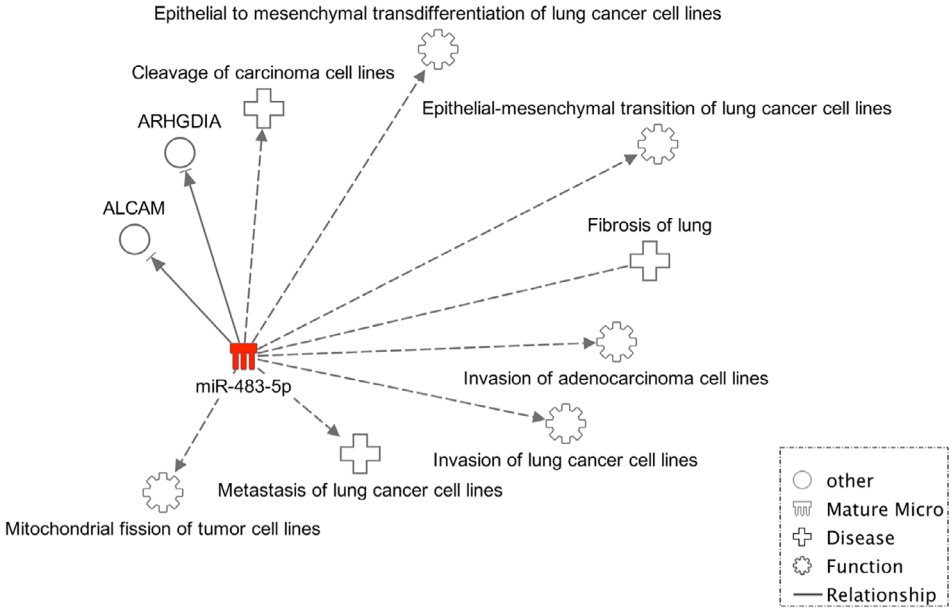

Figure 4 Relationship generated by the Ingenuity Pathway Analysis program (IPA). The shown associations among the microRNA (miR)-483-5p, and the diseases and functions have been selected as related to lung diseases and functions. A solid line represents a direct interaction between miR-483-5p, and the gene products and a dotted line means there is an indirect interaction.

expression of alveolar involvement, airspace edema, interstitial thickening and fibrin deposition at the bronchiolar level.

GGO%, as already evidenced in the literature, is the first and most common feature in the early CT evaluation of COVID-19 pneumonia, whereas in later stages, LC% appears more frequently and has become an index of disease severity.[30]

The positive correlation between GGO% and miR-483-5p at early stages might be attributed to the activation of immunity, and the overexpression of miR-483-5p might underscore the robustness of the immune response associated with a higher percentage of GGO% in the early stages.

It is reasonable to assume that the intensity of the early immune response, along with the increase of GGO%, could contribute to a higher percentage of lung consolidation (LC%) at a later stage, which has been associated with a worse prognosis in both early and later stages according to existing literature.[7,25–27,31]

Interestingly, we did not find any association between miR-483-5p and lung consolidation, a parameter frequently associated with disease severity and prognosis in COVID-19 pneumonia. This lack of correlation could be attributed to various factors. One possibility is that miR-483-5p might play a more significant role in the early stages of lung involvement, as reflected by GGOs, rather than in the later stages characterized by consolidation. This hypothesis aligns with existing literature, which suggests that GGO is the predominant feature in the early evaluation of COVID-19 pneumonia, whereas lung consolidation becomes more prevalent in later stages and is indicative of disease severity.[23,26] Therefore, miR-483-5p might primarily reflect the activation of immune responses associated with GGOs, rather than the later processes reflected by lung consolidation.

The main limitation of the present study was the small sample size, which might limit the generalization of the findings and the ability to detect statistical significance. Other limitations include the observational and retrospective design of the study, and the absence of a longitudinal assessment to examine changes over time in the radiological parameters and miR levels. Further studies

with larger sample sizes and a longitudinal approach are needed to explore the precise role of miR-483-5p and other miRs in the context of lung involvement and disease progression in COVID-19.

In conclusion, the assessment of inflammation, as expressed by miR-483-5p, and the degree of lung involvement, as indicated by CT features, appears to be a promising tool for the prognostic evaluation of COVID-19 pneumonia in older patients. Integrating these measures might provide a better understanding of the different expressions of the disease and contribute to improving patient outcomes.

Acknowledgements

This work was supported by the Gruppo di Ricerca Intradipartimentale Servizi e Tecnologie (GRIST), of the Department of Services and Technologies of IRCCS INRCA, Ancona, Italy.

Funding information

This work was supported by the Italian Ministry of Health (Ricerca Corrente to IRCCS INRCA and Istituti Clinici Scientifici Maugeri IRCCS) and Università Politecnica delle Marche (RSA Grant).

Disclosure statement

The authors declare no conflict of interest.

Author contributions

GB, FO and ADP conceptualized the present study; SC, MDR, LF, SM, GM, LZ, MC, RG, RR, FM and JS collected, analyzed and interpreted the data; VM and MM performed IPA analysis; AC, RS, AC, ARB, DF and EP interpreted the results, commented on and revised successive drafts of the manuscript; SC, MDR, AG and GB were responsible for drafting the manuscript; the manuscript was reviewed by all authors. Finally, all authors read and approved the final manuscript for publication.

Data availability statement

The data that support the findings of this study are available from the corresponding author upon reasonable request.

References

1 Alves VP, Casemiro FG, Araujo BG *et al*. Factors associated with mortality among elderly people in the COVID-19 pandemic (SARS-CoV-2): a systematic review and meta-analysis. *Int J Environ Res Public Health* 2021; **18**: 8008. https://doi.org/10.3390/ijerph18158008.
2 Faraji J, Metz GAS. Aging, social distancing, and COVID-19 risk: who is more vulnerable and why? *Aging Dis* 2021; **12**: 1624–1643. https://doi.org/10.14336/AD.2021.0319.
3 Knopp P, Miles A, Webb TE *et al*. Presenting features of COVID-19 in older people: relationships with frailty, inflammation and mortality. *Eur Geriatr Med* 2020; **11**: 1089–1094. https://doi.org/10.1007/s41999-020-00373-4.
4 Miyashita N, Nakamori Y, Ogata M, Fukuda N, Yamura A. Functional outcomes in elderly patients with hospitalized COVID-19 pneumonia: a 1 year follow-up study. *Influenza Other Respi Viruses* 2022; **16**: 1197–1198. https://doi.org/10.1111/irv.13033.
5 Garg M, Prabhakar N, Bhalla AS *et al*. Computed tomography chest in COVID-19: when & why? *Indian J Med Res* 2021; **153**: 86–92. https://doi.org/10.4103/ijmr.IJMR_3669_20.
6 Hani C, Trieu NH, Saab I *et al*. COVID-19 pneumonia: a review of typical CT findings and differential diagnosis. *Diagn Interv Imaging* 2020; **101**: 263–268. https://doi.org/10.1016/j.diii.2020.03.014.
7 Jayachandran AK, Nelson V, Shajahan ME. Chest CT severity score as a predictor of mortality and short-term prognosis in COVID-19. *J Family Med Prim Care* 2022; **11**: 4363–4367. https://doi.org/10.4103/jfmpc.jfmpc_209_22.
8 Francone M, Iafrate F, Masci GM *et al*. Chest CT score in COVID-19 patients: correlation with disease severity and short-term prognosis. *Eur Radiol* 2020; **30**: 6808–6817. https://doi.org/10.1007/s00330-020-07033-y.
9 Mohamed HA, Abdelkafy AE, Khairy RMM, Abdelraheim SR, Kamel BA, Marey H. MicroRNAs and cytokines as potential predictive biomarkers for COVID-19 disease progression. *Sci Rep* 2023; **13**: 3531. https://doi.org/10.1038/s41598-023-30474-6.
10 Gao L, Kyubwa EM, Starbird MA *et al*. Circulating miRNA profiles in COVID-19 patients and meta-analysis: implications for disease progression and prognosis. *Sci Rep* 2023; **13**: 21656. https://doi.org/10.1038/s41598-023-48227-w.
11 de Gonzalo-Calvo D, Benitez ID, Pinilla L *et al*. Circulating microRNA profiles predict the severity of COVID-19 in hospitalized patients. *Transl Res* 2021; **236**: 147–159. https://doi.org/10.1016/j.trsl.2021.05.004.
12 Giannella A, Riccetti S, Sinigaglia A *et al*. Circulating microRNA signatures associated with disease severity and outcome in COVID-19 patients. *Front Immunol* 2022; **13**: 968991. https://doi.org/10.3389/fimmu.2022.968991.
13 Giuliani A, Matacchione G, Ramini D *et al*. Circulating miR-320b and miR-483-5p levels are associated with COVID-19 in-hospital mortality. *Mech Ageing Dev* 2022; **202**: 111636. https://doi.org/10.1016/j.mad.2022.111636.
14 Jin X, Wang Y, Xu J *et al*. Plasma cell-free DNA promise monitoring and tissue injury assessment of COVID-19. *Mol Genet Genomics* 2023; **298**: 823–836. https://doi.org/10.1007/s00438-023-02014-4.
15 Kustanovich A, Schwartz R, Peretz T, Grinshpun A. Life and death of circulating cell-free DNA. *Cancer Biol Ther* 2019; **20**: 1057–1067. https://doi.org/10.1080/15384047.2019.1598759.
16 Han DSC, Lo YMD. The nexus of cfDNA and nuclease biology. *Trends Genet* 2021; **37**: 758–770. https://doi.org/10.1016/j.tig.2021.04.005.
17 Storci G, Bonifazi F, Garagnani P, Olivieri F, Bonafe M. The role of extracellular DNA in COVID-19: clues from inflamm-aging. *Ageing Res Rev* 2021; **66**: 101234. https://doi.org/10.1016/j.arr.2020.101234.
18 Cheng AP, Cheng MP, Gu W *et al*. Cell-free DNA tissues of origin by methylation profiling reveals significant cell, tissue, and organ-specific injury related to COVID-19 severity. *Med* 2021; **2**: 411–422.e5. https://doi.org/10.1016/j.medj.2021.01.001.
19 Cardelli M, Pierpaoli E, Marchegiani F *et al*. Biomarkers of cell damage, neutrophil and macrophage activation associated with in-hospital mortality in geriatric COVID-19 patients. *Immun Ageing* 2022; **19**: 65. https://doi.org/10.1186/s12979-022-00315-7.
20 Rockwood K, Song X, MacKnight C *et al*. A global clinical measure of fitness and frailty in elderly people. *CMAJ* 2005; **173**: 489–495. https://doi.org/10.1503/cmaj.050051.
21 Hansell DM, Bankier AA, MacMahon H, McLoud TC, Muller NL, Remy J. Fleischner society: glossary of terms for thoracic imaging. *Radiology* 2008; **246**: 697–722. https://doi.org/10.1148/radiol.2462070712.
22 Pan F, Ye T, Sun P *et al*. Time course of lung changes at chest CT during recovery from coronavirus disease 2019 (COVID-19). *Radiology* 2020; **295**: 715–721. https://doi.org/10.1148/radiol.2020200370.
23 Grassi R, Cappabianca S, Urraro F *et al*. Chest CT computerized aided quantification of PNEUMONIA lesions in COVID-19 infection: a comparison among three commercial software. *Int J Environ Res Public Health* 2020; **17**: 6914. https://doi.org/10.3390/ijerph17186914.
24 Li JH, Liu S, Zhou H, Qu LH, Yang JH. starBase v2.0: decoding miRNA-ceRNA, miRNA-ncRNA and protein-RNA interaction networks from large-scale CLIP-Seq data. *Nucleic Acids Res* 2014; **42**: D92–D97. https://doi.org/10.1093/nar/gkt1248.
25 Zakariaee SS, Salmanipour H, Naderi N, Kazemi-Arpanahi H, Shanbehzadeh M. Association of chest CT severity score with mortality of COVID-19 patients: a systematic review and meta-analysis. *Clin Transl Imaging* 2022; **10**: 663–676. https://doi.org/10.1007/s40336-022-00512-w.
26 Li K, Wu J, Wu F *et al*. The clinical and chest CT features associated with severe and critical COVID-19 pneumonia. *Invest Radiol* 2020; **55**: 327–331. https://doi.org/10.1097/RLI.0000000000000672.

27 Li Y, Yang Z, Ai T, Wu S, Xia L. Association of "initial CT" findings with mortality in older patients with coronavirus disease 2019 (COVID-19). *Eur Radiol* 2020; **30**: 6186–6193. https://doi.org/10.1007/s00330-020-06969-5.
28 Zhang X, Guo J, Fan S *et al*. Screening and identification of six serum microRNAs as novel potential combination biomarkers for pulmonary tuberculosis diagnosis. *PLoS One* 2013; **8**: e81076. https://doi.org/10.1371/journal.pone.0081076.
29 Huang S, Feng C, Zhai YZ *et al*. Identification of miRNA biomarkers of pneumonia using RNA-sequencing and bioinformatics analysis. *Exp Ther Med* 2017; **13**: 1235–1244. https://doi.org/10.3892/etm.2017.4151.
30 Churruca M, Martinez-Besteiro E, Counago F, Landete P. COVID-19 pneumonia: a review of typical radiological characteristics. *World J Radiol* 2021; **13**: 327–343. https://doi.org/10.4329/wjr.v13.i10.327.
31 Colombi D, Villani GD, Maffi G *et al*. Qualitative and quantitative chest CT parameters as predictors of specific mortality in COVID-19 patients. *Emerg Radiol* 2020; **27**: 701–710. https://doi.org/10.1007/s10140-020-01867-1.

Supporting Information

Additional supporting information may be found in the online version of this article at the publisher's website:

Table S1. High-predicted and moderate-predicted mRNA targets of miR-483-5p. The analysis was performed using the microRNA target filter analysis by IPA.

Table S2. Coefficients of the correlation between radiological parameters and circulating biomarkers.

How to cite this article: Cecchini S, Di Rosa M, Fantechi L, et al. Relationship between imaging-derived parameters and circulating microRNAs to study the degree of lung involvement in hospitalized geriatric patients with COVID-19 pneumonia. Geriatr. Gerontol. Int. 2024;1–11. https://doi.org/10.1111/ggi.14940